Dusty plasma induced by solar radiation under microgravitational conditions: an experiment on board the Mir orbiting space station

V. E. Fortov, A. P. Nefedov, O. S. Vaulina,*) A. M. Lipaev, V. I. Molotkov,
A. A. Samaryan, V. P. Nikitskiĭ, A. I. Ivanov, S. F. Savin, A. V. Kalmykov,
A. Ya. Solov'ev, and P. V. Vinogradov

*Scientific-Research Center for the Thermal Physics of Pulsed Effects, Russian Academy of Sciences, 127412
Moscow, Russia*

The dynamics of the formation of ordered structures of macroparticles charged by photoemission under the action of solar radiation under microgravitational conditions without the use of electrostatic traps to confine the particles is studied experimentally and theoretically. The working conditions needed for the formation of structures of charged macroparticles are chosen as a result of a numerical solution of the problem posed, the particle charges and the interparticle interaction parameter are determined, and the characteristic times specifying the dynamics of the formation of an ordered system of macroparticles are calculated. The behavior of an ensemble of macroparticles under the effect of solar radiation is observed experimentally on board the Mir space station. An analysis and comparison of the results of the experimental and theoretical investigations permit drawing a conclusion regarding the possibility of the existences of extended ordered formations of macroparticles charged by photoemission under microgravitational conditions. © *1998 American Institute of Physics.* [S1063-7761(98)00712-4]

1. INTRODUCTION

Space research has revealed the importance of dust and dust structures in the formation of stars, planetary systems, and planetary rings, in processes occurring in the upper layers of the atmosphere (the magnetosphere and ionosphere), etc.[1–3] One of the mechanisms for charging dust particles under the conditions of outer space in the presence of intense fluxes of ultraviolet radiation is photoemission. As a result of this process, macroparticles measuring several microns can acquire a positive charge of the order of $10^2 - 10^5$ electron charges.[4] On the other hand, under the conditions of a low-pressure gas discharge, the strong interparticle correlation resulting from the large values of the macroparticle charge (of the order of $10^2 - 10^5$ electron charges) leads to the formation of ordered structures in the arrangement of the macroscopic particles, which are similar to the structures in a liquid or a solid.[5–11] The principal mechanism for charging particles immersed in a radio-frequency (rf) or dc discharge relies on electron and ion fluxes. Because of the higher temperature and mobility of electrons, the particle charge is negative.

One common feature of this group of experiments is the fact that the ordered structures observed do not have a free boundary, since they are confined by the electric field of a striation or the electrodes in the earth's gravitational field and by the potential well formed by the field of the rf discharge or the floating potential of the walls of the gas-discharge vessel in the horizontal direction, respectively. Experiments involving the observation of ordered structures of positively charged cerium oxide particles in a laminar jet of a weakly ionized thermal plasma are exceptions.[11–14]

A plasma with positively charged particles can also form as a result of photoemission when particles are irradiated in a buffer gas by a flux of photons with an energy exceeding the work function of a photoelectron escaping from their surface. Under certain conditions (particle size and concentration, wavelength and intensity of the UV radiation, and photoelectron work function) crystalline structures can appear in such a system.[4,11] The characteristic value of the photoelectron work function for most substances does not exceed 6 eV; therefore, photons with an energy $\leqslant 12$ eV can charge particles without ionizing a buffer gas, such as He or Ar.

Three principal mechanisms can be singled out among the mechanisms by which dust acquires a positive charge. They are the thermionic emission, photoemission, and secondary emission of electrons from the surfaces of dust particles, which, along with charging by electrons, can play a significant role both in the formation of cosmic dust structures and in processes occurring in the upper layers of the atmosphere. The existence of different mechanisms for charging dust in outer space can cause the agglomeration and growth of particles due to the electrostatic attraction of dust particles with opposite charges[15,16] or lead to the formation of plasma-dust structures with a predominant contribution of one of the mechanisms for charging macroparticles under consideration. The investigation of such structures is promising from the standpoint of both basic science and technological applications. It is noteworthy that the possibility of studying plasma-dust crystals with free boundaries can be realized most fully only under the conditions of weightlessness or microgravitation.[17] The study of the formation of ordered structures of charged macroparticles under microgravitational conditions yields new information, which can-
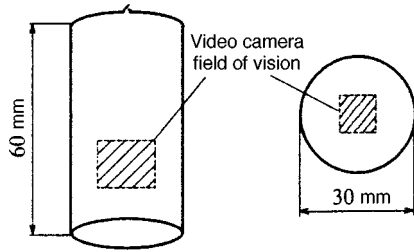
FIG. 1. Geometric dimensions of the working chamber.

not be obtained under laboratory conditions on earth.

The purpose of performing the space experiment was to study the possibility of the existence of plasma-dust structures in the upper layers of the earth's atmosphere when the particles are charged by solar radiation as a result of the photoemission of electrons from their surface. The working conditions needed for the formation of structures of charged macroparticles in the experimental chamber (the type of buffer gas and its pressure, as well as the concentration, material, and size of the particles) were selected as a result of a preliminary numerical analysis of the problem posed; the particle charges induced by solar radiation and the interparticle interaction parameter were determined, and the times specifying the dynamics of the formation of an ordered system of macroparticles (the charging time, braking time, and dispersion times of particles in the working chamber and the times for establishing ordered dust structures) under microgravitational conditions without the use of electrostatic traps to confine the particles were calculated. The calculations were performed for particles of different materials and sizes (1–100 μm) with variation of their concentration and the pressure of the buffer gas.

Experimental investigations of the behavior of an ensemble of macroparticles charged by solar radiation were performed under microgravitational conditions on board the Mir space station.

2. FORMATION OF ORDERED STRUCTURES OF MACROPARTICLES UNDER THE ACTION OF SOLAR RADIATION

2.1. Photoemission charging of particles

Let us consider macroparticles in a neutral gas being irradiated by a source, whose emission has an intensity and a spectral composition corresponding to the characteristics of solar radiation with consideration of the spectral transmission coefficient of the illuminator, the air layer, and the window of the working chamber (Fig. 1) with the particles under investigation.

The conditions for the formation of ordered structures of macroparticles induced by the effects of solar radiation are investigated using particles of cerium oxide (CeO_2), particles of lanthanum boride (LaB_6), and spherical particles of a bronze with a cesium coating. The choice of these particle materials is specified by the efficiency of their photoemission charging and low adhesion, so that the particles under investigation would not adhere to one another and would not precipitate on the walls of the working chamber. The reference data on the quantum efficiency Y of the particle materials in the near-UV and visible regions of the spectrum, the work function W for photoemission, and the densities ρ of the particle materials are listed in Table I, which also indicates the size (radius) r_p and initial concentration n_p of the particles. The initial concentration n_p of the particles is determined by the condition of transparency of the disperse system to the external photoinducing radiation, on the one hand, and the possibility of achieving the maximum values of the interparticle interaction parameter Γ, on the other hand. Taking into account the optical characteristics (the refractive index and sizes) of the particles investigated, we can estimate the optical density τ of the disperse layer as

$$\tau \approx 2\pi r_p^2 n_p H, \tag{1}$$

where r_p is the particle radius and H is the height of the vessel with the particles. The interparticle interaction parameter Γ can be written as a function of the particle concentration n_p in the form

$$\Gamma = (Ze)^2 (4\pi n_p/3)^{1/3}/T_g. \tag{2}$$

Here $l = (4\pi n_p/3)^{-1/3}$ is the mean distance between particles, Z is the particle charge, and T_g is the temperature of the particles, which is equal to the temperature of the buffer gas ($\simeq 0.03$ eV). Thus, an optical density $\tau \approx 1$, which permits achievement of the maximum values of Γ with lowering of the radiation intensity roughly by a factor of $e \approx 2.78$, was selected as a criterion for selecting the value of n_p. The initial particle concentration was determined from (1) as

$$n_p \approx 1/2\pi r_p^2 H. \tag{3}$$

The mass of the particle load in the vessel was calculated from the volume of the vessel (see Fig. 1), the required concentration n_p, and the mass of an individual particle with the mean radius r_p (Table I). The results of experimental investigations of the behavior of CeO_2, LaB_6, and bronze particles under low-pressure conditions (0.01–100 Torr) were also taken into account. More specifically, because of the agglomeration of CeO_2 and LaB_6 particles and their precipitation on the vessel wall, the particle concentration in the working volume decreases by roughly an order of magni-

TABLE I. Values of the radius r_p and the initial concentration n_p of particles with a material of density ρ, the quantum yield Y, the work function W, the limiting particle charge Z_{max} (4), the interparticle interaction parameter Γ_{max} (2), and the effective photon flux density J (6) of solar radiation.

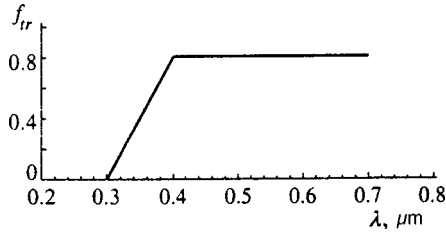| Particles	r_p, μm	ρ, g/cm^3	W, eV	Y	J, photons/cm^2	n_p, 1/cm^3	Z_{max}, e	Γ_{max}
CeO_2	0.5–1.5	7.3	3	10^{-2}	1.33×10^{16}	7.0×10^6	7.8×10^2	4.2×10^2
LaB_6	1–5	2.6	2	10^{-2}	9.16×10^{16}	7.2×10^6	4.5×10^3	1.4×10^4
Bronze	25–50	8.2	1.5	10^{-4}	1.72×10^{17}	5.6×10^3	6.9×10^4	6.5×10^5

FIG. 2. Spectral transmission function $f_{tr}(\lambda)$ of the device.

tude. Values of n_p ten times smaller than the table values were used to estimate the mean distance between these particles (CeO$_2$, LaB$_6$) and Γ_{max} (Table I). The bronze particles did not adhere to one another when the vessel was evacuated, and the table value of the particle concentration corresponds to the basic theoretical parameter n_p.

The limiting (maximum) charges Z_{max} of the particles following the photoemission of electrons from their surface and the value of the interparticle interaction parameter Γ_{max} can be estimated from the condition of equality between the surface potential ϕ_s and the quantity $h\nu_{max} - W$ as

$$Z_{max} = (h\nu_{max} - W)r_p/e, \qquad (4)$$

where $h\nu_{max}$ is the maximum photon energy, which corresponds in our case to a wavelength $\lambda_{min} \approx 0.3 \ \mu m$ and is determined by the transmission function f_{tr} of the experimental vessel (the transmission of the quartz illuminator, the air layer, and the glass of the working window of the vessel). The dependence of the approximating transmission function f_{tr} of the apparatus on the wavelength λ used in the further calculations is shown in Fig. 2. The values of Z_{max} obtained from Eq. (4) and the values of Γ_{max} obtained from Eq. (2) are listed in Table I. It can easily be seen that the value of Γ and the charge of the particles increase with their size. However, the selection of large particles with $r_p > 100 \ \mu m$ for performing the experiments is undesirable, since it requires lowering the initial particle concentration n_p [see (3)] to values that are unsuitable for observation.

Let us estimate the value of the charge of the particles when they are irradiated by a source with a solar spectrum, taking into account that the plasma-dust system under consideration consists of positively charged macroparticles and photoelectrons emitted by them. The positive potential of the particles is established as a result of the balance between the recombination of electrons on a particle surface and the photoemission electron flux from the particle surface. In the case of a dilute plasma (with a concentration of neutrals $n_n \leq 10^{14} \ cm^{-3}$), in which the mean free path l_e of photoelectrons before collisions with neutrals greatly exceeds the particle radius r_p ($l_e \gg r_p$), the balance equation can be written in the following form:[4]

$$4n_e\left(\frac{T_e}{2\pi m_e}\right)^{1/2}\left(1 + \frac{e\phi_s}{T_e}\right) = YJ\exp\left(-\frac{e\phi_s}{T_{pe}}\right), \qquad (5)$$

where m_e is the electron mass, n_e and T_e are the electron concentration in the bulk of the plasma and the electron temperature, J is the photon flux density, Y is the quantum yield of photoelectrons, and T_{pe} is their mean energy. It is assumed

here that the efficiency of the absorption of UV radiation is close to unity. The temperature T_{pe} of the electrons leaving a particle surface upon photoemission depends on the particle material and lies in the range from 1 to 2 eV in most cases.[18,19] Assuming that the rate of electron recombination on the particles exceeds the rate of thermal energy loss due to collisions with neutrals, we can set $T_{pe} \approx T_e$.

In order to determine the equilibrium charge $Z = \phi_s r_p/e$ of the particles under investigation in the working chamber and to estimate the dust charging time, we must calculate the integral number J of solar photons that are capable of causing the photoemission of electrons from a particle surface and estimate the concentration n_e of electrons returning to the particle surface. To calculate the photon flux density J, solar radiation was simulated by a black body with a temperature of 5800 K.[19] The calculation was performed using the formula

$$J = \int_{\lambda_{min}}^{\lambda_{max}} \frac{f_{tr}c_1\lambda^{-4}d\lambda}{\{\exp(c_2/\lambda T_c) - 1\}hc}, \qquad (6)$$

where f_{tr} is the transmission function of the experimental chamber (Fig. 2), $\lambda_{min} = 0.3 \ \mu m$, and λ_{max}, i.e., the red edge of the photoeffect, is determined by the work function W for the particle material. The results of the calculations of J for the particles investigated are presented in Table I.

The concentration n_e of electrons returning to the particle surface can be obtained from the solution of the problem of an infinite cylinder uniformly charged throughout its volume. The distributions of the field $E(r)$ and the potential $\phi(r)$ in such a cylinder are specified by the following relations

$$E(r) = 2\pi\sigma r, \qquad (7a)$$

$$\phi(r) = \pi\sigma(R_{cyl}^2 - r^2) + \phi_{wall}, \qquad (7b)$$

where $\sigma = e(Zn_p - n_e) = en_e^{wall}$ is the space-charge density and ϕ_{wall} is the potential of the wall of a cylinder of radius R_{cyl}. The floating potential of the surface of the vessel wall ϕ_{wall} is then determined by the photoelectrons escaping from the particles, and the field appearing in the ampul does not allow all the electrons emitted to leave the particle system. The concentration n_e^{wall} of electrons reaching the ampul wall can be estimated from the relation $T_{pe} \approx e\Delta\phi$, where $e\Delta\phi = e\phi_{av} - e\phi_{wall}$ is the mean energy lost by electrons in the electric field of the vessel. According to the mean-value theorem, from (7b) we have

$$\phi_{av} = \phi_{wall} - \pi\sigma R_{cyl}^2/3.$$

The concentration n_e of electrons remaining in the volume under investigation can be written as

$$n_e = Zn_p - n_e^{wall} \simeq Zn_p - 3T_{pe}/\pi e^2 R_{cyl}^2. \qquad (8)$$

An estimate of the value of n_e^{wall} for photoelectrons with a temperature $T_{pe} = 1-2$ eV gives $n_e^{wall} \simeq 5 \times 10^6 \ cm^{-3}$ in a vessel with a radius $R_{cyl} = 1.5$ cm. The values of Z and Γ calculated on the basis of the values of n_e^{wall} and J obtained are listed in the first row for each type of particle in Table II,

TABLE II. Values of the interparticle interaction parameter Γ and the particle charge Z_p calculated from the balance equation (5) for various values of the macroparticle concentration n_0.

Particles	n_0, cm^{-3}	Z, e	Γ
	10^6	3	10^{-2}
CeO$_2$	10^5	28	3.0×10^{-2}
	10^4	212	7.5
	10^6	14	1.5×10^{-1}
LaB$_6$	10^5	131	6.2
	10^4	785	10^2
	10^3	2672	5.5×10^2
Bronze	10^3	5090	2.0×10^3
	10^2	50 070	9.0×10^4

TABLE III. Values of the natural frequency ω_0 of charged macroparticles for an initial concentration n_0, the braking time τ_{br}, the drift times of the particles to the vessel wall for lowering the initial particle concentration n_0 by factors of 10 (t_{td1}) 100 and (t_{td2}), and the time for establishing short-range order t_{str} for various values of the pressure P.

Particles	P, Torr	n_0, cm^{-3}	ω_0, s^{-1}	τ_{br}, s	t_{td1}, s	t_{td2}, s	t_{str}, s
	0.01	10^6	67.7	1.25	0.023	0.061	0.015
CeO$_2$		10^5	21.4		0.074	0.192	0.047
	70	10^6	67.7	1.8×10^{-4}	3.64	40	0.12
		10^5	27.4		36.4	400	1.21
	0.01	10^6	124.8	1.32	0.013	0.033	0.008
LaB$_6$		10^5	39.5		0.040	0.110	0.025
	70	10^6	124.8	1.9×10^{-4}	1.01	11.14	0.034
		10^5	39.5		10.1	111.4	0.337
	0.01	10^3	0.778	52	2.00	5.28	1.28
Bronze		10^2	0.246		6.41	16.71	4.06
	40	10^3	0.778	0.13	38.11	419.1	1.27
		10^2	0.246		381.1	4191	12.7

which corresponds to a particle concentration $n_p=n_0$ in the vessel. It should be noted that $n_e\neq0$ only if the initial particle concentration n_0 satisfies the condition

$$n_0 Z_{max} < n_e^{wall}.$$

Otherwise, the space-charge density in formulas (7a) and (7b) is defined as $\sigma = e Z_{max} n_0$.

The results of the calculations presented in this section allow us to postulate the possibility of the formation of crystal- or liquid-type ordered structures of macroparticles for assigned illumination conditions ($h\nu_{max}$ and J) and macroparticle parameters (W, Y, r_p, and n_0). However, it should be noted that the presence of electrons from the external plasma or photoelectrons returning to the particle surfaces can significantly lower the charge Z of the macroparticles and the value of Γ. In the general case the condition for transparency of the macroparticle cloud to emitted or ''external'' electrons is close to the condition for transparency of the disperse system to the external radiation source causing photoelectron emission from the particle surfaces.

2.2. Characteristic times specifying the dynamics of the formation of dust structures

The possibility of observing ordered structures of macroparticles induced by solar radiation in an experimental chamber with finite dimensions (Fig. 1) is determined by the characteristic times specifying the dynamics of the formation of an ordered system of macroparticles. We shall estimate the charging time, the braking time, the times for establishing ordered macroparticle structures, and the dispersion time of particles in the working chamber with a buffer gas at two different pressures. Neon was selected as the buffer gas for performing the investigations because of its chemical inertness toward the material and cesium coating of the particles, its spectral transparency, and its high ionization potential. The choice of the two different buffer gas pressures (0.01 and 40–70 Torr) was dictated by the possibility of observing the dynamics of the formation of ordered structures for different particle charge values (see Sec. 2.1).

The charging time τ_{ch} of the macroparticles can be determined from the time needed for a particle to acquire the charge $Z=Z_{max}$ by solving the following differential equation:

$$\frac{dZ}{dt} = \pi r^2 \left\{ 4n_e \left(\frac{T_e}{2\pi m_e} \right)^{1/2} \left(1 + \frac{e\phi_s}{T_e} \right) \right.$$

$$\left. - YJ \exp\left(-\frac{e\phi_s}{T_{pe}} \right) \right\}. \tag{9}$$

The solution of (9) for both $n_e^{wall}\simeq5\times10^6$ cm^{-3} and $n_e\simeq0$ when the particles are charged to $Z=Z_{max}$ gives $\tau_{ch}<10^{-5}$ s under our conditions.

The braking times τ_{br} of macroparticles in a vessel with two different values of the pressure P are listed in Table III. The braking times τ_{br} for all the particles, except the bronze particles at the ''high'' pressure, were calculated in the free-molecule approximation.[20] The value of τ_{br} for the bronze particles at $P=40$ Torr was determined within the Stokes approximation (the viscosity regime).[21]

The dispersion time of particles in a vessel can be obtained from a numerical molecular-dynamics analysis of the dynamics of the particle system. To investigate the variation of the concentration of charged macroparticles as a function of time, we solved the equation of motion with and without consideration of the thermal (Brownian) motion of the particles:

$$m_d \frac{d^2 \mathbf{r}_k}{dt^2} = \sum_j \left. \Phi(r) \right|_{r=|\mathbf{r}_k-\mathbf{r}_j|} \frac{\mathbf{r}_k - \mathbf{r}_j}{|\mathbf{r}_k - \mathbf{r}_j|} - m_d \nu \frac{d\mathbf{r}_k}{dt} + \mathbf{F}_B. \tag{10}$$

Here m_d is the mass of a particle, and $\Phi(r)$ is the interparticle interaction parameter. For a Coulomb interaction this quantity can be represented in the form

$$\Phi(r) = \frac{(eZ)^2}{r^2}, \tag{11}$$

where r is the distance between two interacting particles. In the our case Debye screening can be neglected, since the system under consideration is not electroneutral, and the Debye radius is greater than the mean distance between the
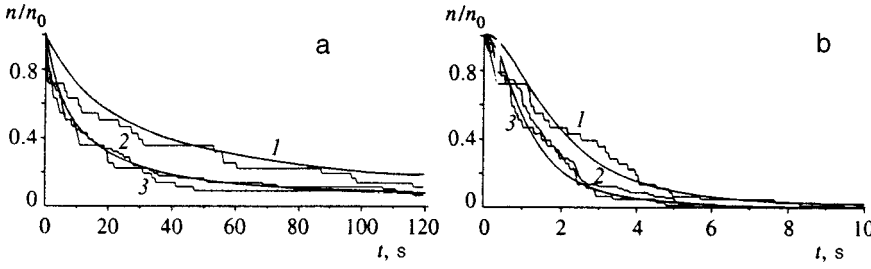
FIG. 3. Molecular-dynamics plots of the concentration $n(t)/n_0$ (solid line) as a function of the time t at the pressures $P=40$ (a) and 0.01 Torr (b) for various values of the initial frequency ω_0: 1 — $\omega_0=0.32$ s^{-1}, $n_0=165$ cm^{-3}, $Z=69\,000$; 2 — $\omega_0=0.53$ s^{-1}, $n_0=465$ cm^{-3}, $Z=69\,000$; 3 — $\omega_0=0.53$ s^{-1}, $n_0=165$ cm^{-3}, $Z=110\,400$. The smooth lines show approximations based on formulas (14a) (a) and (14b) (b).

particles. The system of equations (10) and (11) was solved for a transverse section of a cylindrical vessel with consideration of the absorption of charged macroparticles on the walls under the condition that the particle velocity is equal to zero at the initial moment in time. An analysis of the solution of Eqs. (10) and (11) for the cases of high $[\nu=(\tau_{br})^{-1}\gg1]$ and low $(\nu\leqslant1)$ buffer-gas pressures allowed us to conclude that the relative variation of the particle concentration $n(t)/n_0$ as a function of the time t is determined by the natural frequency ω_0 at $t=0$:

$$\omega_0=\sqrt{\frac{(Ze)^2n_0}{m_d}}, \tag{12}$$

where $n_0=n(t=0)$. The values of ω_0 are given in Table III for various initial concentrations of macroparticles of different materials with the charge $Z=Z_{max}$. In addition, it was found that thermal motion of the particles does not have a significant influence on their dynamic characteristics (dispersion times and correlation functions) at kinetic temperatures K of the particles up to $K=10-50$ eV. Plots of n/n_0 as a function of time are presented in Figs. 3a and 3b for various values of ω_0 and bronze particles with the charge $Z=Z_{max}$ in a gas with high $P=40$ Torr, (Fig. 3a) and low $P=0.01$, (Fig. 3b) pressures.

In order to find an approximation of $n(t)/n_0$ for different values of ω_0, we solved the equation of motion for two charged particles:

$$\frac{d^2r}{dt^2}=-\nu\frac{dr}{dt}+\left(\frac{Ze}{r}\right)^2\frac{1}{m_d}. \tag{13}$$

Here $\nu=(\tau_{br})^{-1}$ is the friction coefficient. Equation (13) was solved for the case of high pressures $(\nu\gg1)$ in the diffusion approximation with the left-hand side of the equation equal to zero. In the case of low pressures $(\nu\leqslant1)$ the friction coefficient in (13) was set equal to zero $(\nu=0)$. This allowed us to obtain the following relations for approximating $n(t)/n_0$:

$$n(t)/n_0=(1+3\omega_0^2t/\nu)^{-1}, \quad \nu\gg1, \tag{14a}$$

$$n(t)/n_0=8(1+\sqrt{1+4\omega_0^2t^2})^{-1}, \quad \nu\leqslant1. \tag{14b}$$

The approximations of $n(t)/n_0$ found are also presented in Figs. 3a and 3b for the corresponding values of ω_0. The functions (14a) and (14b) permit the determination of ω_0 from the results of an experiment in which the macroparticle charge can be obtained for a known concentration n_0 at a certain moment in time $t=0$. The minimum dispersion time of particles of different materials with the charge $Z=Z_{max}$

was estimated on the basis of the dependences obtained. The drift times of the particles to the vessel wall determined from formulas (14a) and (14b) for lowering the initial particle concentration n_0 by factors of 10 (t_{td1}) and 100 (t_{td2}) are listed in Table III for various initial conditions.

The time for establishing ordered macroparticle structures t_{str} in a vessel at low and high buffer-gas pressures can be specified on the basis the solution of (10) and (13) by the following conditions:

$$t_{str}\gg\omega, \quad \nu\leqslant1, \tag{15a}$$

$$t_{str}\approx\nu/\omega^2, \quad \nu\gg1, \tag{15b}$$

where $\omega=\sqrt{(Ze)^2n/m_d}$ is the natural frequency of the charged particles in the structure. The molecular-dynamics calculations show that the times for establishing short-range order correspond to $t_{str}\propto\omega_0$ ($\nu\leqslant1$) and $t_{str}\propto0.1\nu/\omega_0^2$ ($\nu\gg1$). These values of t_{str} are listed in Table III for various initial concentrations of particles with the charge $Z=Z_{max}$ and buffer-gas pressures P.

The results of the calculations show that the drift time t_{td} of the particles to the vessel wall is shorter in all the cases considered than the time t_{ch} for photoemission charging of the particles and the time t_{str} for establishing a liquid-type macroparticle structure. Thus, it can be concluded that short-range correlation orders of interparticle distances (liquid-type dust structures) can be observed under microgravitational condition without the use of electrostatic traps to confine the particles. To illustrate the dynamics of the formation of ordered macroparticle structures under these conditions, Figs. 4a and 4b present the results of a molecular-dynamics calculation of pair-correlation functions for bronze particles with a charge $Z_{max}=69\,000$ in a buffer gas (neon) at different pressures. The dashed lines denote correlation functions corresponding to the time t_{str} for the formation of short-range order. The figure also shows fragments of the spatial configuration of the particles in the initial moment in time and at the time $t(n_0/n=10)$ for a decrease in the initial particle concentration $n_0=165$ cm^{-3} by an order of magnitude.

3. EXPERIMENT

3.1. Experimental setup

The experiment was carried out on a setup consisting of the following principal units (Fig. 5):

1. a working chamber;
2. interchangeable glass ampuls containing particles of lanthanum boride LaB_6 (two ampuls), bronze with a cesium
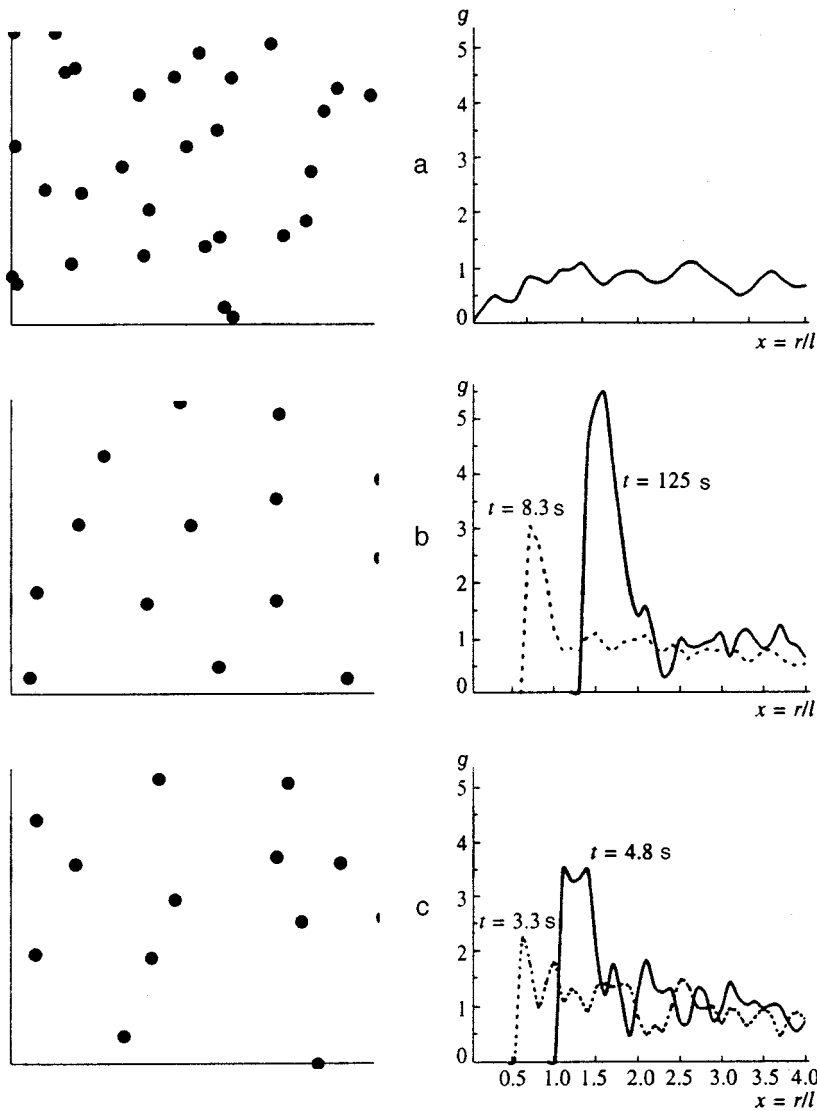
FIG. 4. Fragments of the spatial configuration of the particles and the pair-correlation functions $g(x)$ (where $x = r/l$) for bronze particles with $Z = 69\,000$ in a buffer gas with different values of the pressure P at various moments in time t: a — $t = 0$ s; b — $P = 40$ Torr, $t = 125$ s; c — $P = 0.01$ Torr, $t = 4.8$ s. The dashed lines show the correlation functions corresponding to the time t_{str} for the formation of short-range order.
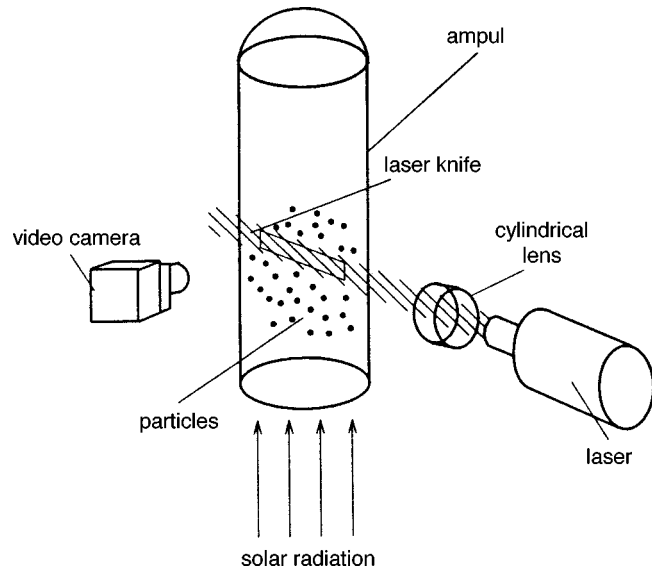

FIG. 5. Schematic representation of the experimental setup.

monolayer (two ampuls), and cerium oxide CeO_2 (two ampuls) in a buffer gas (neon) at different pressures;

3. radiation source — a 30-mW semiconductor laser with a working wavelength of 0.67 μm;

4. a ''Glisser'' television system, including a power supply, an ordinary CCD camera with an objective lens, a tape-recorder module, and a remote-control panel;

5. supports.

The interchangeable glass ampuls had the form of glass cylinders, one of whose end surfaces was a flat uviol glass window and was intended for illuminating the particles with solar radiation (Fig. 1). Immediately before the performance of an experiment, the required ampul was placed in the clamp of the working-chamber holder with its flat end surface toward the illuminator. For diagnostics of the ensemble of particles, the ampul was illuminated by a flat laser beam (a ''laser knife;'' the width of the ''knife'' was no greater than 200 μm), and an image was obtained using the CCD camera, whose signal was recorded on magnetic tape. The field of vision of the video camera had the form of a rectangle measuring roughly 8×10 mm (Fig. 1). The camera was aimed at the center of the ampul (see Fig. 1), and the
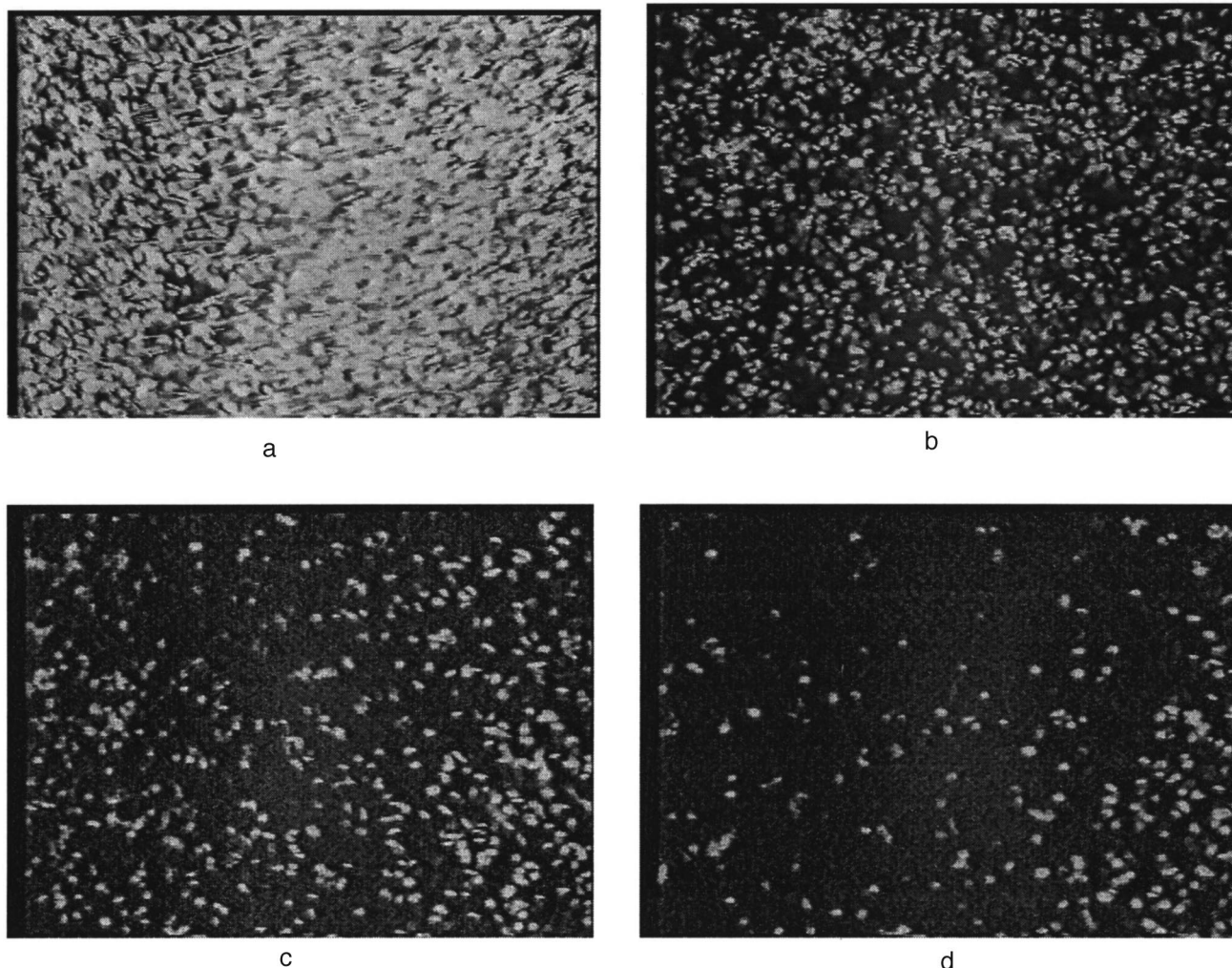
FIG. 6. Successive states of the system of bronze particles in the ampul with $P_1 = 0.01$ Torr following dynamic disturbance of the system.

depth of focus for the f stop of 16 chosen was about 10 mm. The experiments were carried out with three values of the working pressure: $P_1 = 0.01$ Torr (for all the types of particles investigated), $P_2 = 40$ Torr (for the bronze particles), and $P_3 = 70$ Torr (for the LaB_6 and CeO_2 particles).

3.2. Behavior of a macroparticle substructure under microgravitational conditions

The first stage of the experiment was confined to observing the behavior of the ensemble of macroparticles placed in the working chamber under the action of solar radiation. In the initial state the particles were on the walls of the ampul; therefore, the experiment was carried out according to the following scheme: a dynamic disturbance (jolt) of the system and relaxation to the initial state, i.e., drift to the wall. The experiments showed that the investigations can be performed only with bronze particles, since the cerium oxide and lanthanum boride particles are incompletely shaken from the walls, rapidly agglomerate, and adhere to the vessel wall, darkening the working region. Therefore, the further analysis was performed only for the bronze particles.

Figures 6a–6d show the successive states of the system

of particles in the ampul with $P_1 = 0.01$ Torr following dynamic disturbance of the system, and Figs. 7a–7d show the state of the system in the ampul with $P_2 = 40$ Torr. Observations of the motion of the particles showed that the velocity vectors of the particles are randomly directed in the initial stage and that the particles drift to the walls without a preferential direction. Subsequently, a preferential direction usually appears, but motion along definite trajectories is displayed more strongly in the vessel with the higher pressure (see Fig. 7). Vibration of the particles on a background of the overall translational motion was observed in several experiments, and the treatment of the particle trajectories revealed periodic variations of the magnitude of the particle velocity in all the experiments. These variations of the particle velocity can be associated with fluctuations of the particle charge or with the dynamic action of microscopic accelerating forces arising on board the space station. Variation of the visibility of the particles was observed (one possible cause is rotation). One more interesting finding is the formation of agglomerates, in which the number of particles varies from three or four to several hundred (Figs. 8a and 8b). These agglomerates can depart from the vessel walls in response to
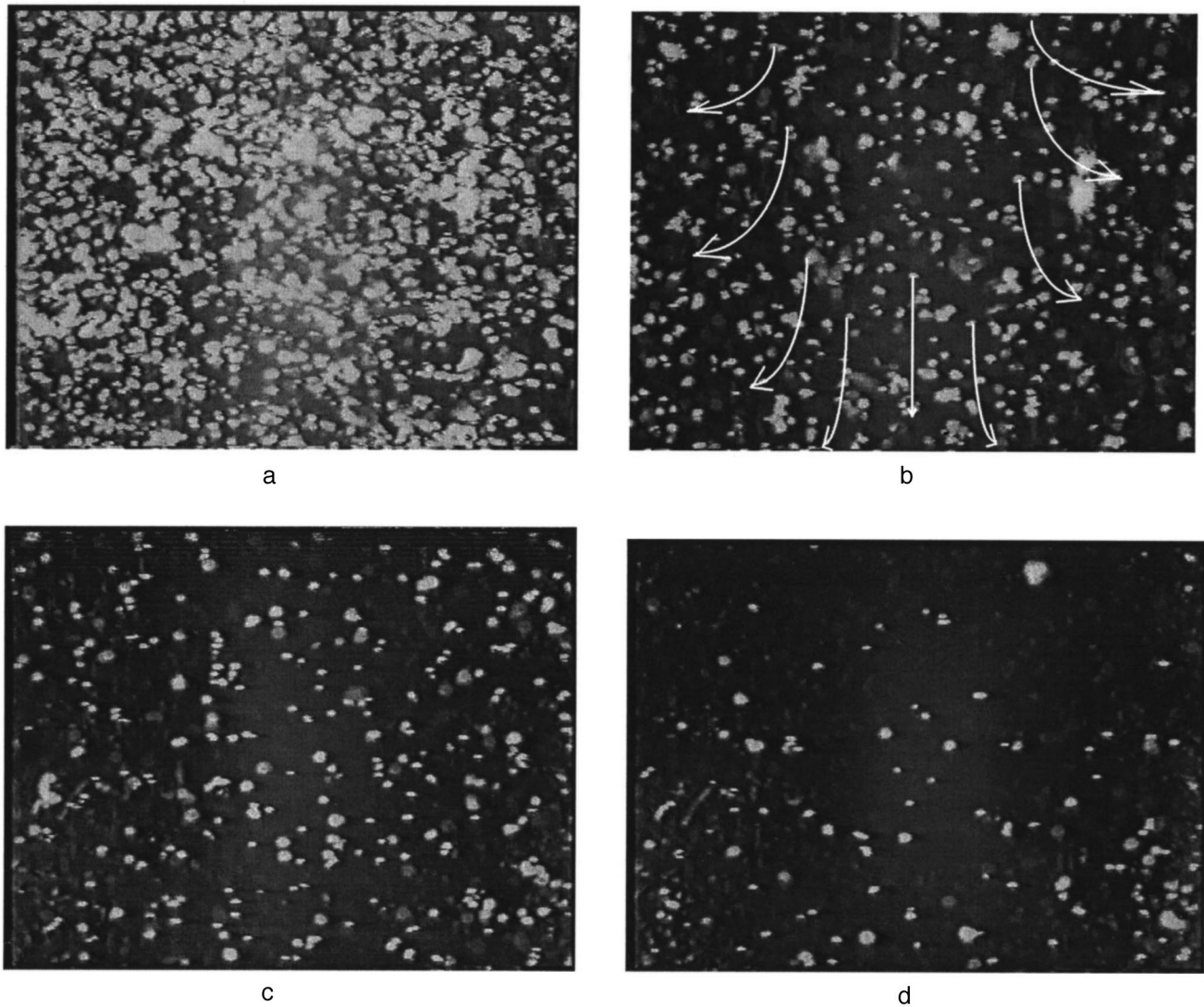
FIG. 7. Successive states of the system of bronze particles in the ampul with $P_1 = 40$ Torr following dynamic disturbance of the system.

a weak dynamic disturbance. The results of the observations of the behavior of the particles in the vessel with the higher pressure show that the bulk of the agglomerates form in the volume of the vessel during a period of a few seconds following the dynamic disturbance. The agglomeration of particles in the volume of the vessel may occur because the particles acquire opposite charges in the initial moments of illumination: positive charges are acquired as a result of the emission of photoelectrons, and negative charges are imparted by the fluxes of electrons emitted from neighboring particles. A similar effect was observed in Ref. 15.

It was concluded that particles are charged on the basis of observations of the changes in the trajectories of the particles when they come close to one another (collide) or approach the wall. It should also be noted that the particles move very slowly in the vessel with $P_2 = 40$ Torr when the solar radiation is blocked and that acceleration of the motion occurs when radiation acts on the ensemble of particles. The charge of the macroparticles can be estimated by analyzing their dynamic behavior.

3.3. Determination of the particle charge

According to observations of the behavior of ensembles of particles during illumination, the drift time of the particles to the wall was about 5 s for $P_1 = 0.01$ Torr and from 3 to 5 min in the vessel with the buffer-gas pressure $P_2 = 40$ Torr. This suggests (according to the data in Table III) that the bronze particles were charged to a level close to the theoretical value $Z_{\max} = 69\,000$. The particle charge can be estimated both from the relative variation of the concentration of the particles and from their trajectories of motion. In the first case approximations of the types (14a) and (14b), which permit the determination of ω_0 from experimental plots of the relative variation of the particle concentration $n(t)/n_0$, can be used to determine the particle charge. Figures 9a and 9b present experimental plots of $n(t)/n_0$ and the approximating functions (14a) and (14b) with $\omega_0 = 0.315$ s^{-1} which give the best agreement with experiment both for the case of $P_2 = 40$ Torr and for the vessel with the lower pressure $P_1 = 0.01$ Torr.

a
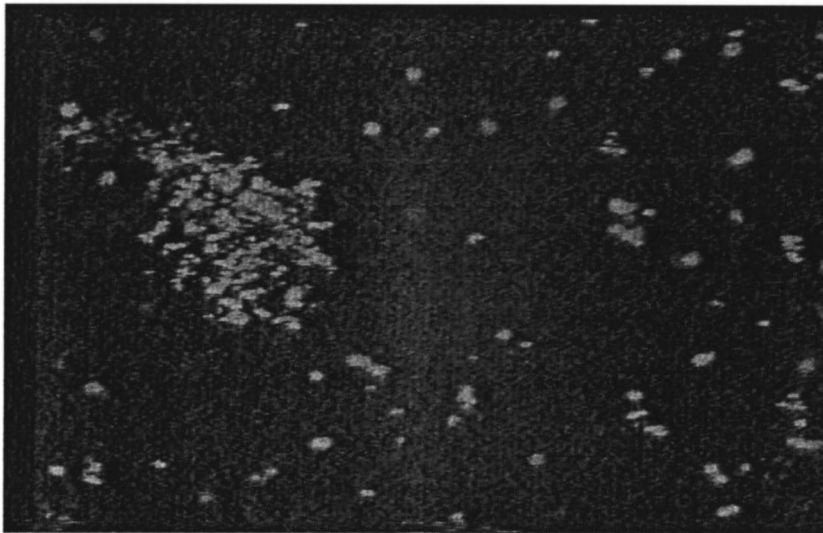
FIG. 8. Formation of macroparticle agglomerates.

b

The plots of $n(t)/n_0$ were determined during illumination by solar radiation following a period of holding in the dark, during which the particles managed to lower the velocity acquired from the initial jolt (Figs. 9a and 9b). In the case of shaking the vessel while it is exposed to solar radiation, it is very difficult to interpret the experimental data (see Fig. 9), since it is virtually impossible to determine the initial particle concentration n_0 to the required accuracy. The initial concentration n_0 was determined in the absence of solar radiation from the number of particles falling in the plane of

the laser knife and ranged from 150 to 250 cm^{-3}. On the basis of the values found $n_0 = 150-250$ cm^{-3} and $\omega_0 = 0.315$ s^{-1}, the particle charge can be specified as

$$Z = (\omega_0/e)\sqrt{m_d/n_0} = (6.38 \pm 0.81) \times 10^4.$$

Thus, the charge obtained corresponds to $Z_{\max} = 69\,000$ to within 13%.

The second method for determining the particle charge is
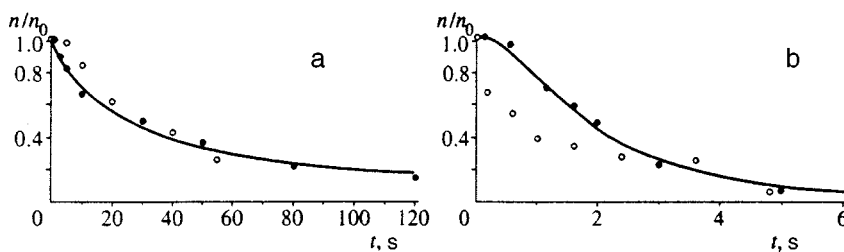

FIG. 9. Experimental plots of the concentration $n(t)/n_0$ as a function of the time t in vessels with pressures equal to 40 (a) and 0.01 Torr (b) obtained at times $t \gg \tau_{\mathrm{br}}$ following dynamic disturbance of the vessel (filled circles) and immediately after agitation of the vessel (unfilled circles). The solid lines show the approximations (14a) and (14b) for the natural frequency $\omega_0 = 0.315$ s^{-1}.

TABLE IV. Results of the determination of the charge Z of particles from their trajectories of motion.

No.	P, Torr	n_p, cm^{-3}	a, m/s^2	V, m/s	Z
1		10^1	6×10^{-4}	2.5×10^{-3}	5×10^4
2	0.01	3×10^1	1.2×10^{-3}	6×10^{-3}	10^5
3		5×10^1	1.6×10^{-3}	1.2×10^{-2}	8×10^4
4	40	3×10^1	1.5×10^{-4}	7×10^{-5}	3×10^4

based on solution of the equation of motion of a particle in a known electric field $E(r)$:

$$\frac{d^2r}{dt^2} = -\nu\frac{dr}{dt} + E\frac{Ze}{m_d}. \tag{16}$$

The electric field intensity E can be assigned by Eq. (7) with consideration of averaging over the radius of the cylinder as $E = \pi e Z n_p R_{\text{cyl}}$. Here we take into account that the space-charge density is $\sigma = e Z n_p$ for $Z n_p < n_e^{\text{wall}}$ and $\sigma = e n_e^{\text{wall}}$ for $Z n_p > n_e^{\text{wall}}$, since the motion of the particles was analyzed at low concentrations ($n_p < 10^2$). After determining the velocity V and the acceleration a of the particles from their trajectories of motion, the particle charge can be found from Eq. (16):

$$Z^2 = a m_d/(e^2\pi n_p R_{\text{cyl}}), \quad P_1 = 0.01 \text{ Torr}, \tag{17a}$$

$$Z^2 = (V+a)m_d/(e^2\tau_{\text{br}}\pi n_p R_{\text{cyl}}), \quad P_2 = 40 \text{ Torr}. \tag{17b}$$

Table IV presents the characteristic values of the macroparticle charges, which agree well with the value of the charge obtained from the variation of the relative particle concentration $n(t)/n_0$. It is noteworthy that the slight upward deviation of the charge in the low-pressure case can easily be explained, since lighter particles and, accordingly, smaller particles having a smaller charge leave the vessel volume first under low-viscosity conditions. In the high-viscosity case the drift time of the particles to the wall should not depend strongly on their size.

Despite the high particle charges and the large value of the interaction parameter $\Gamma \simeq 10^4$ (see Table IV), no strong correlation between the interparticle distances could be observed. The measured correlation functions exhibit appreciable deviations for the calculated curves (Fig. 4). The typical form of the correlation functions obtained as a result of the treatment of experimental images without illumination (the laser knife) and with solar irradiation is shown in Fig. 10. The difference between the experimental and calculated
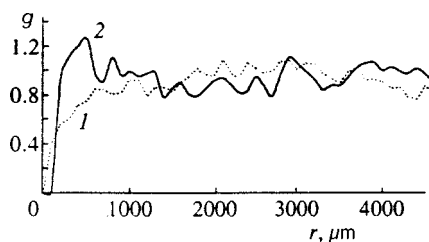
results can be due to several factors: polydispersity of the particle powder investigated and the formation of agglomerates, in which the number of particles varies from three or four to several hundred. The latter factor makes a highly significant contribution to breakdown of the correlation of the interparticle distances.

4. CONCLUSION

The results of observations of the behavior of an ensemble of macroparticles charged by photoemission under the action of solar radiation under microgravitational conditions have been presented. The particle charges have been estimated, and it has been established that the particles are charged to the maximum possible levels, i.e., several units times 10^4, under the conditions of the experiment. The results of a calculation of the particle charges due to photoemission correspond to the results of the observations. The particle charges have been estimated by two methods, which provide good agreement with the calculation: from the trajectories of motion of the particles and with the use of the approximations obtained for the variation of the relative particle concentration. The values of the charges and the interparticle interaction parameter obtained demonstrate the possibility of the formation of ordered crystal- and liquid-type macroparticle structures under the conditions studied. It is noteworthy that under the conditions of outer space the charging efficiency of particles with a low photoelectron work function is higher due to the additional effect of the UV portion of the solar spectrum and that the interparticle interaction parameter consequently increases.

Although the dynamic behavior of the particles (the variation of the particle concentration in the volume investigated) corresponds well to the behavior determined as a result of a numerical analysis, the form of the experimentally observed correlation functions differs strongly from the theoretical form and attests to the formation of only weakly correlated liquid-type structures. The principal cause of this difference may be the agglomeration of oppositely charged particles during charging. Nevertheless, an analysis and comparison of the results of the experimental and theoretical investigations confirm the conclusion that the existence of extended liquid-type ordered formations of macroparticles charged by solar radiation is possible under microgravitational conditions even if there is substantial agglomeration of the particles.

*)E-mail: ipdustp@redline.ru

FIG. 10. Experimental correlation functions $g(r)$ obtained as a result of the treatment of images without illumination (*1*) and with solar irradiation (*2*).

[1] S. A. Kaplan, *Interstellar Medium and the Origin of Stars*, [in Russian], Znanie, Moscow (1977).
[2] N. N. Gor'kavyĭ and A. M. Fridman, Usp. Fiz. Nauk **160**, 169 (1990) [Sov. Phys. Usp. **33**(2), 95 (1990)].
[3] F. Melanso and O. Havnes, J. Geophys. Res. **95**, 5837 (1991).
[4] M. Rosenberg and D. A. Mendis, IEEE Trans. Plasma Sci. **23**, 177 (1995).
[5] V. E. Fortov, A. P. Nefedov, V. M. Torchinsky, V. I. Molotkov, O. F. Petrov, A. A. Samarian, A. M. Lipaev, and A. G. Khrapak, Phys. Lett. A **229**, 317 (1997).
[6] J. H. Chu and I. Lin, Phys. Rev. Lett. **72**, 4009 (1994).

[7] H. Thomas, G. E. Morfill, V. Demmel *et al.*, Phys. Rev. Lett. **73**, 652 (1994).

[8] Y. Hayashi and K. Tachibana, J. Phys. Soc. Jpn. **33**, L804 (1994).

[9] A. Melzer, T. Trottenberg, and A. Piel, Phys. Lett. A **191**, 301 (1994).

[10] V. E. Fortov, A. P. Nefedov, V. M. Torchinskiĭ, V. I. Molotkov, A. G. Khrapak, O. F. Petrov, and K. F. Volykhin, JETP Lett. **64**, 92 (1996).

[11] A. P. Nefedov, O. F. Petrov, and V. E. Fortov, Usp. Fiz. Nauk **167**, 1215 (1997) [Phys. Usp. **40**, 1163 (1997)].

[12] V. E. Fortov, A. P. Nefedov, O. F. Petrov, A. A. Samarian, and A. V. Chernyschev, Phys. Rev. E **54**, 2236 (1996).

[13] V. E. Fortov, A. P. Nefedov, O. F. Petrov, A. A. Samarian, and A. V. Chernyschev, Phys. Lett. A **219**, 89 (1996).

[14] V. E. Fortov, A. P. Nefedov, O. F. Petrov, A. A. Samaryan, and A. V. Chernyshev, Zh. Éksp. Teor. Fiz. **111**, 467 (1997) [JETP **84**, 256 (1997)].

[15] T. Yokota and K. Honda, J. Quant. Spectrosc. Radiat. Transf. **56**, 761 (1996).

[16] C. Cui and J. Goree, Trans. Plasma Sci. **22**, 151 (1994).

[17] V. N. Tsytovich, Usp. Fiz. Nauk **167**, 57 (1997) [Phys. Usp. **40**, 53 (1997)].

[18] C. K. Goertz, Geophys. Rev. **27**, 271 (1989).

[19] V. A. Grilikhes, P. P. Orlov, and L. B. Popov, *Solar Energy and Space Flights* [in Russian], Nauka, Moscow (1986).

[20] I. T. Yakubov and A. G. Khrapak, Sov. Tech. Rev. B Therm. Phys. **2**, 269 (1989).

[21] D. V. Sivukhin, *General Course in Physics* [in Russian], Nauka, Moscow (1979), Vol. 1, p. 496.

Translated and edited by P. Shelnitz